

# Stress Transfer at the Nanoscale on Graphene Ribbons of Regular Geometry

*A.C. Manikas<sup>1,2</sup>, M.G. Pastore Carbone<sup>1</sup>, C. R. Woods<sup>3</sup>, Y. Wang<sup>3</sup>, I. Souli<sup>1</sup>, G. Anagnostopoulos<sup>1</sup>, M. Hadjinicolaou<sup>4</sup>, K. S. Novoselov<sup>3</sup> and C. Galiotis<sup>1,2\*</sup>*

*<sup>1</sup>Institute of Chemical Engineering, Foundation for Research and Technology Hellas (ICEHT/FORTH), Stadium St., Platani, 26504, Patras, Greece*

*<sup>2</sup>Department of Chemical Engineering, University of Patras, Patras 26504, Greece*

*<sup>3</sup>School of Physics and Astronomy, University of Manchester, Manchester, U.K*

*<sup>4</sup>Hellenic Open University, Science & Technology, Patras, Greece*

## Figures

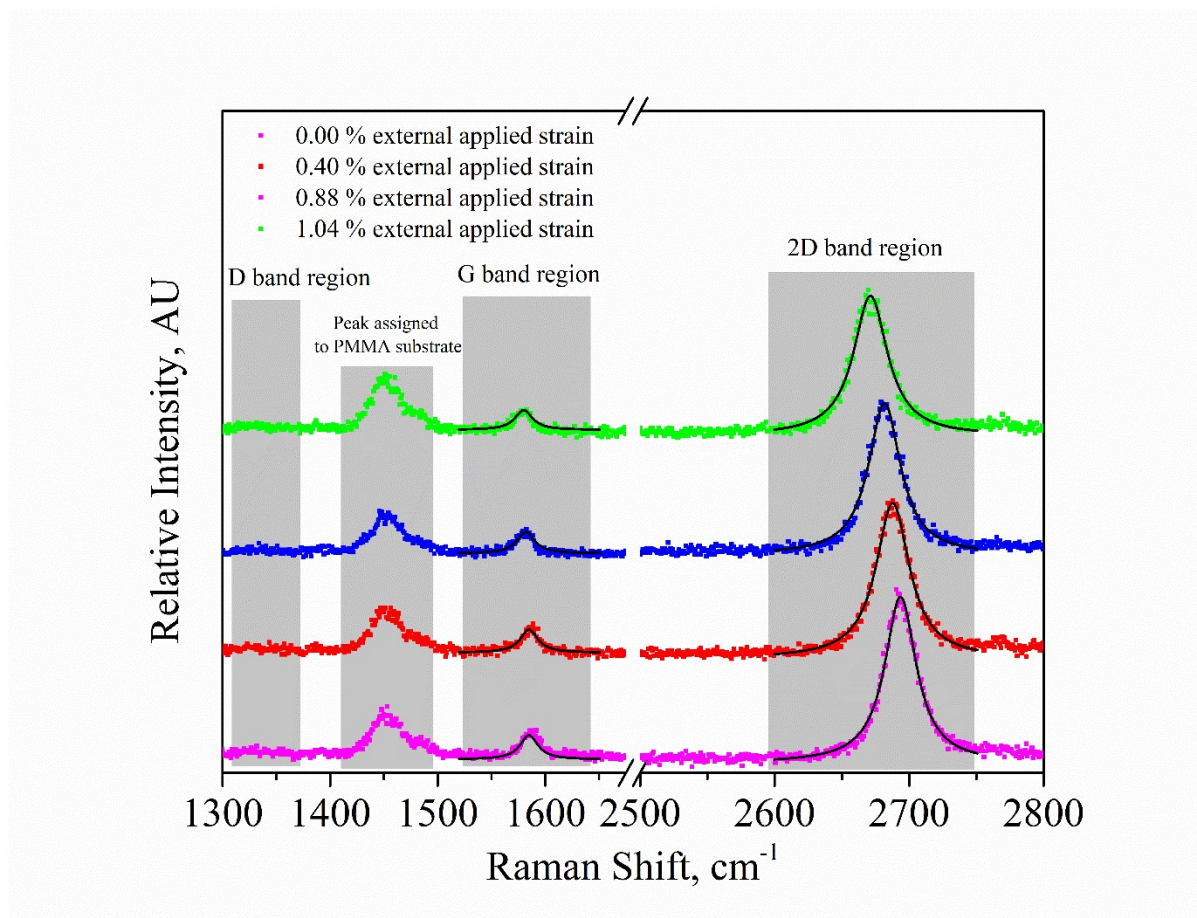


**Figure S1.** Representative Raman spectra of the embedded graphene micro-ribbons collected at different strain levels. It is highlighted the representative graphene G, 2D and D band regions and the PMMA band region with the characteristic peaks. In all the cases no D peak is observed. The solid lines represent Lorentzian fits to the G and 2D peak.

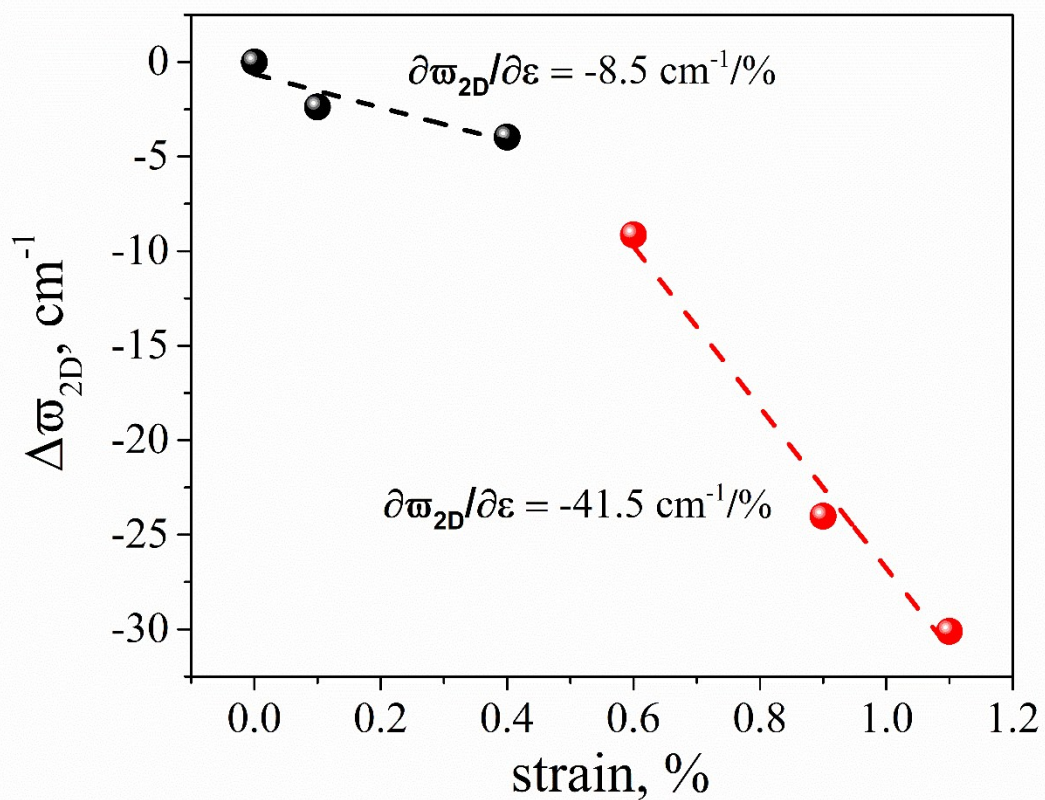


**Figure S2.** 2D peak position for spectra acquired far away from the edge as a function of applied strain during the 2<sup>nd</sup> loading. Two regions are marked: i) an almost flat region corresponding to the unfolding of the pre-existing wrinkles of the inclusion with, ii) linear region where graphene experiences axial tensile load.

## Stress dependence on graphene's Raman spectrum

It is well known that phenomena like overtones, combination bands, bond breaking at high deformation levels cannot be explained with the harmonic vibrator theory and demands a different approximation to the potential energy. Such an approximation is the Morse potential function that is presenting in the following equation:

$$U = D_e(1 - e^{-b(x-x_0)})^2 \quad (22)$$

Where  $D_e$  is the dissociation energy and  $b$  is a constant.

In Figure S3, the potential energy of both the anharmonic and harmonic oscillator is presented with the allowable energy levels. The dotted lines represent the allowable energy levels.

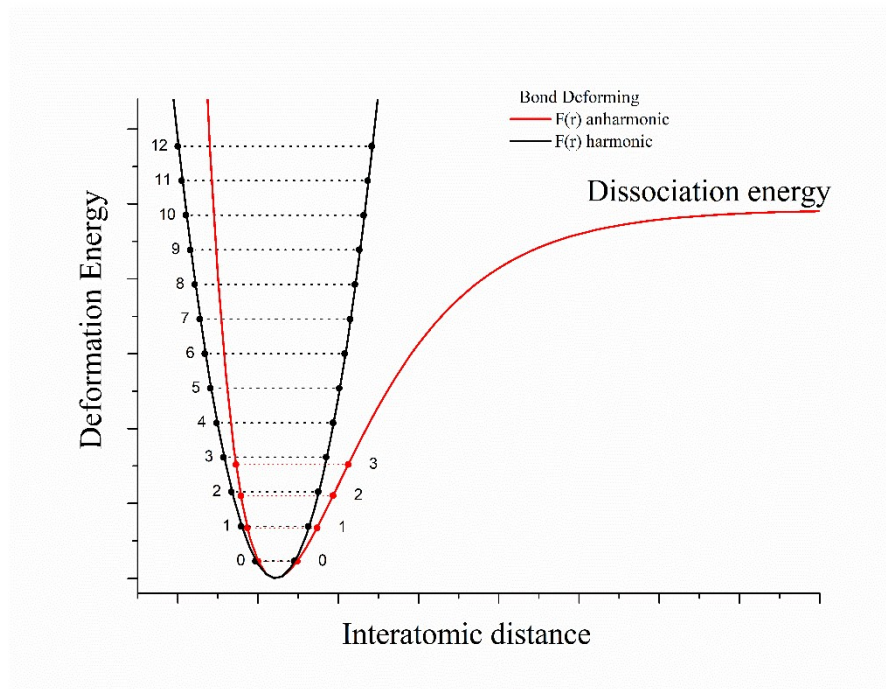


**Figure S3.** The potential energy function for the Harmonic and the Anharmonic Oscillator as a function with the interatomic distance with the allowable energy levels.

The second derivative from potential energy provides the force constant in both cases. More detailed, in the harmonic oscillator the force constant is stable and equal to  $K$  but in the anharmonic oscillator the force constant is given from the following equation:

$$K = 2b^2 D_e \left( 2e^{-2b(x-x_0)} - e^{-b(x-x_0)} \right) \quad (23)$$

In figure S4, the force constant for anharmonic and harmonic oscillator is presented. It can be easily seen that the force constant is no more constant in the anharmonic case and it is a function of the intermolecular distance. More detailed, when the bond is stressed,  $\Delta x > 0$  the force constant is decreasing. This results in a low frequency shift  $\Delta \nu$  of the vibration. On the other hand, when the bond is compressed,  $x < 0$ , the force constant increasing resulting a high frequency shift. For small deformations (positions near the equilibrium),  $\Delta \nu \sim \sqrt{K}$ . The above principle provides the theoretical background for the frequency shift of distinct Raman bands when the molecule is subjected to external load.

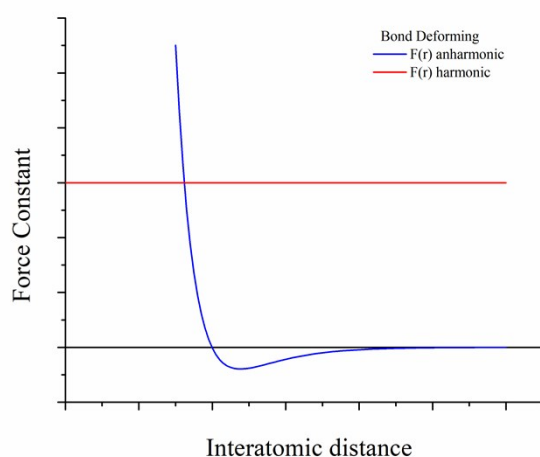


**Figure S4.** The variation of the force constant as a function of interatomic distance for harmonic and anharmonic oscillator cases.

## **Monitoring stress transfer processes using micro Raman spectroscopy**

Raman spectroscopy provides a unique insight into the relationship between macroscopic deformation and the processes that occur at the molecular or microstructural level and has now revolutionized common understanding of the micromechanics of inclusions in composite materials. It has been found that the frequencies or wavenumbers of the Raman bands of many high-performance fibres (e.g. Kevlar) and carbon-based materials shift on the application of an external mechanical loading. This behaviour has been ascribed to the macroscopic deformation being transformed directly into stressing of the covalent bonds and changes in the bond angles<sup>1</sup>. As a consequence of the anharmonicity of atomic bond, when an external loading is applied to a material, the interatomic distance changes thus resulting in a variation of the interatomic force and of vibrational frequency (or, analogously, in wavenumber). Based on this approach, Galiotis et al. used for the first time the inclusion of a composite as a ‘mechanical probe’ for a polydiacetylene/epoxy composite<sup>2</sup>. Basically, this approach consists in monitoring in situ the Raman vibrational frequencies shift with applied stress or strain for the matrix-embedded inclusion and to compare this dependence with a universal calibration curve established between the rate of shift of a specific Raman bands of the inclusion with applied strain. In the same way, the point-to-point mapping along inclusion axis enables stress transfer from the polymer to the inclusion to be followed.

**Mathematical formulation for the stress transfer of a nanoflake such as graphene simply supported or embedded into a polymer matrix.**

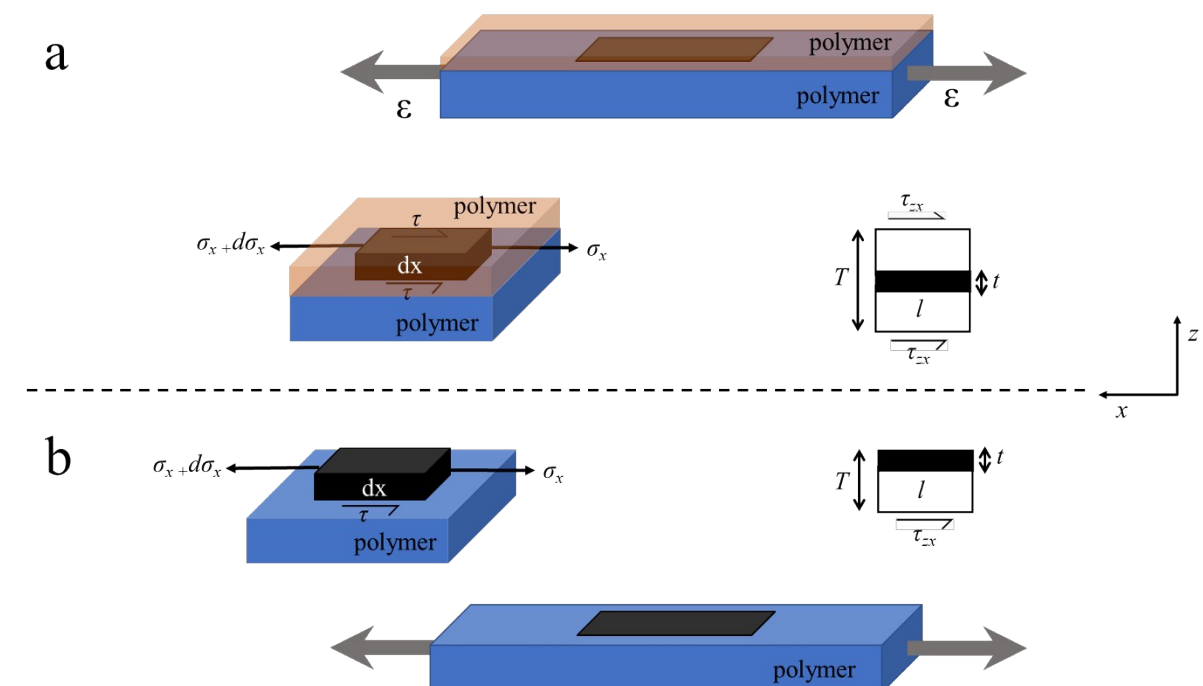


**Figure S5** Geometry of the shear lag model in (a) fully embedded and (b) simply supported graphene flake on a polymeric bar. Axial and shear stresses in representative elements of the flake are also shown.

The shear-lag formulation presented here is a modification of the treatment proposed by Cox<sup>3</sup> for a composite that incorporates say a rectangular graphene monolayer of length,  $l$ , width,  $w$ , and of thickness,  $t_g$ , which is either simply supported or embedded into a solid polymer matrix. The fundamental material assumptions of the model are that the inclusion (flake, platelet, fibre etc) is surrounded by a matrix (or even bounded by a matrix on the one side), that there is a reasonable adhesion exists between the inclusion and the matrix and that both inclusion and matrix behave elastically. Finally, no load transfer across the ends of the

inclusion (normal to the cross-section) is permitted in this model. If the whole matrix is subjected to a strain  $\varepsilon$  in the direction of the flake, the rate of load,  $P$ , from matrix to the flake, will depend on the magnitude of the relative displacement of the two bodies i.e. the reinforcing flake at  $u_x$  (the distance  $x$  is measured from the end) and the far-field displacement of the matrix  $u_{x,\infty}$  at the same point. In other words:

$$\frac{dP}{dx} = H(u_x - u_{x,\infty}) \quad (1)$$

or

$$\frac{d\sigma_x}{dx} = \frac{H(u_x - u_{x,\infty})}{wt_g} \quad (2)$$

where  $H$  is a proportionality constant and  $\sigma_x$  is the axial stress in the flake. In the linear elastic regime,  $\sigma_x$  is given by:

$$\sigma_x = E_x \left( \frac{du_x}{dx} \right) \quad (3)$$

whereas the far field (matrix) strain,  $\varepsilon$ , is given by:

$$\frac{du_{x,\infty}}{dx} = \varepsilon_m \equiv \varepsilon \quad (4)$$

By differentiating equation (2) with respect to  $x$  and by substituting equations (1) and (3) we finally get:

$$\frac{d^2\sigma_x}{dx^2} = \frac{H}{wt} \left( \frac{\sigma_x}{E_x} - \varepsilon \right) \quad (5)$$

The solution of the above differential equation yields:

$$\sigma_x = E_x \varepsilon + R \sinh \beta x + S \cosh \beta x \quad (6)$$



where  $R$ ,  $S$  and  $\beta$  are constants. By considering the boundary conditions:

$$\begin{aligned} x = 0 &\rightarrow \sigma_x = 0 \\ x = l &\rightarrow \sigma_x = 0 \end{aligned} \quad (7)$$

Equation (6) is finally transformed to:

$$\sigma_x = E_x \varepsilon \left[ 1 - \frac{\cosh \left[ \beta \left( \frac{l}{2} - x \right) \right]}{\cosh \left( \beta \frac{l}{2} \right)} \right] \quad (8)$$

where

$$\beta = \sqrt{\left( \frac{H}{wtE_f} \right)} \quad (9)$$

is the shear-lag parameter which depends on the material properties and the geometrical foundation of the problem and  $H$  the proportionality constant. The parameter  $\beta$  has units of inverse length and is evidently related to the transfer length required for efficient transfer of stress to the flake. A simplified version of equation (8) using trigonometric identities is:

$$\sigma_x(x) = E_x \cdot \varepsilon \cdot \left[ 1 - \cosh(\beta x) + \tanh\left(\frac{\beta l}{2}\right) \cdot \sinh(\beta x) \right] \quad (10)$$

Now we turn our attention to the expression  $\beta \cdot \left(\frac{l}{2}\right)$ . Since  $\beta = 1/l_o$  and  $l_o = \left(1 - \frac{1}{e}\right)l_t = 0.63l_t$  then

the function  $\tanh\left(\frac{\beta l}{2}\right) \equiv \tanh\left(0.8 \frac{l}{l_t}\right)$ . Since in this paper we only examine efficient stress

transfer it follows that we need  $l \gg 2l_t$ . Hence the expression  $\tanh\left(\frac{\beta l}{2}\right)$  yields to 0.92 in the limiting case of  $l = 2l_t$  for any higher values of  $l$  it becomes a unity and can be ignored.

Since as mentioned above is  $1/l$  the half-lengths of graphene flakes employed here are in the range of  $\sim 10 \mu\text{m}$  then any value of  $\beta \geq 1.0 \mu\text{m}^{-1}$  (which is our case here) will satisfy this.

Based on the above, equation (10) now becomes:

$$\begin{aligned} \sigma_x(x) &= \sigma_{x,\infty} \cdot [1 - \cosh(\beta x) + \sinh(\beta x)] \\ \text{or} & \\ \sigma_x(x) &= \sigma_{x,\infty} \cdot [1 - \exp(-\beta x)] \end{aligned} \quad (11)$$

where,  $\sigma_{x,\infty}$  is the far-field stress of the flake. In terms of strain values, the above equation can be written as:

$$\varepsilon_x(x) = \varepsilon \cdot [1 - \exp(-\beta x)] \quad (12)$$

The significance of equations (11) and (12) is that the stress or strain distributions in the elastic region can be adequately predicted by just treating  $\beta$  as an *inverse length* fitting parameter which is related to the physics of the stress transfer problem and represents a normalization factor to the length of the inclusion that permits full stress transfer.

In order to estimate the value of  $H$ , we consider the balance of shear to axial forces (Figure S5) in the flake which yields:

$$\frac{d\sigma_x}{dx} = -\frac{2\tau_t}{t_g} \quad (13) \text{ for the fully embedded and}$$

$$\frac{d\sigma_x}{dx} = -\frac{\tau_t}{t_g} \quad (14) \text{ for the simply supported case}$$

where  $\tau_t$  is the shear stress at the surface of the flake. The shear strain  $\gamma$  at the interface should be given by:

$$\gamma_{xz} = \frac{\partial u_x}{\partial z} + \frac{\partial u_z}{\partial x} \quad (15)$$

It is reasonable to assume [4] that :

$$\left| \frac{\partial u_z}{\partial x} \right| \ll \left| \frac{\partial u_x}{\partial z} \right| \quad (16)$$

then equation (15) gives:

$$\gamma = \frac{\partial u_x}{\partial z} = \frac{\tau_{zx}}{G_{m,z}} \quad (17)$$

where  $G_{m,z}$  is the shear modulus of the matrix at distance  $z$  and  $\tau_{zx}$  is the shear stress at any given distance  $z$  from the surface of the flake for which there is no influence of the inclusion.

By considering the balance of shear forces,  $\tau_t$ , at distance  $z$  and those at the flake surface,  $\tau_t$ , over the width of the flake it is easy to show that:

$$\tau_{zx} = \tau_t \quad (18)$$

Equation (17) can be integrated at the limits of the flake surface ( $t/2$ ) for which  $u_x = u_{x,t}$  and of the matrix element ( $T/2$ ) for which  $u_x = u_{x,T}$ :

$$\int_{u_x=u_{x,t}}^{u_x=u_{x,T}} du_x = \frac{\tau_t}{G_{m,T}} \int_{t/2}^{T/2} dz \quad \text{or} \quad (19)$$

$$u_{x,T} - u_{x,t} = \frac{\tau_t}{2G_{m,T}} (T - t_g)$$

where  $G_{m,T}$  is the shear modulus of the matrix at a distance  $T$  (fig. S6). Hence solving as for  $H$  from equations (2), (13) or (14) and (19) (assuming as mentioned earlier  $u_{x,T} = u_{x,\infty}$  and  $T \gg t_g$ ), we obtain:

$$H_{\text{embedded}} = \frac{2wG_{m,T}}{T-t_g}; \frac{2G_{m,T}}{\left(\frac{T}{2}\right)}w \text{ and } H_{\text{simply-supported}}; \frac{G_{m,T}}{\left(\frac{T}{2}\right)}w \quad (20)$$

Equation (20) represents  $H$ , the proportionality constant, as the shear modulus of the ‘interphase’ normalized by its own thickness ( $T/2$ ) and multiplied by the width of the flake. In order now to establish the inverse length parameter for all graphene nanocomposites we set  $t = nt_g$  where  $n$  is the number of layers and  $t_g = 0.335$ , the thickness of the monolayer. In our case, from equations (9) and (20) we obtain:

$$\beta_{\text{embedded}} = \sqrt{\underbrace{\left(\frac{2G_{m,T}}{\left(\frac{T}{2}\right)}\right)}_{\text{INTERPHASE}} \underbrace{\left(\frac{1}{nt_g E_g}\right)}_{\text{GRAPHENE CONSTANTS}}} \text{ and } \beta_{\text{simply-supported}} = \sqrt{\underbrace{\left(\frac{G_{m,T}}{\left(\frac{T}{2}\right)}\right)}_{\text{INTERPHASE}} \underbrace{\left(\frac{1}{nt_g E_g}\right)}_{\text{GRAPHENE CONSTANTS}}} \quad (21)$$

The first term of equations (21) refer to the ‘interphase’, through which the stresses are transferred to graphene, and the second to the material parameters of the nanoflake. The above expression for  $\beta$  agrees well with similar expressions derived by Kotha *et al*<sup>4</sup> for composites reinforced with mineral platelets.

## References

1. Batchelder, D. N.; Bloor, D., STRAIN DEPENDENCE OF THE VIBRATIONAL MODES OF A DIACETYLENE CRYSTAL. *J Polym Sci Polym Phys Ed* **1979**, *17* (4), 569-581.
2. Galiotis, C.; Young, R. J.; Yeung, P. H. J.; Batchelder, D. N., The study of model polydiacetylene/epoxy composites - Part 1 The axial strain in the fibre. *Journal of Materials Science* **1984**, *19* (11), 3640-3648.

3. Cox, H. L., The elasticity and strength of paper and other fibrous materials. *British Journal of Applied Physics* **1952**, 3 (3), 72-79.
4. Kotha, S. P.; Kotha, S.; Guzelsu, N., A shear-lag model to account for interaction effects between inclusions in composites reinforced with rectangular platelets. *Compos. Sci. Technol.* **2000**, 60 (11), 2147-2158.